Thursday, July 3, 2003

An unusual N-terminal deletion of the laminin α3a isoform leads to the chronic granulation tissue disorder laryngo-onycho-cutaneous syndrome.

W. H. Irwin McLean[1,*], Alan D. Irvine[2], Kevin J. Hamill[1], Neil V. Whittock[1], Carrie M. Coleman[1], Jemima E. Mellerio[3], Gabrielle S. Ashton[3], Patricia J. H. Dopping-Hepenstal[3], Robin A. J. Eady[3], Tanvir Jamil[4], Rodney J. Phillips[5], S. Ghulam Shabbir[6], Tahir S. Haroon[6], Khawar Khurshid[6] Jonathan E. Moore[7], Brian Page[7], Jonathan Darling[8], David J. Atherton [9], Colin S. Munro[10], Frances J. D. Smith[1] and John A. McGrath[3].

1. Epithelial Genetics Group, Human Genetics Unit, Department of Molecular and Cellular Pathology, University of Dundee, Ninewells Medical School, Dundee, UK, DD1 9SY

2. Department of Paediatric Dermatology, Our Lady's Hospital for Sick Children, Dublin, Ireland

3. Genetic Skin Disease Group, St John's Institute of Dermatology, The Guy's, King's College and St Thomas' Hospitals' Medical School, St Thomas' Hospital, London, UK

4. Hasham M. Jamil Trust, Burnham Health Centre, Minniecroft Road, Burnham, Burkinghamshire, UK, SL1 7DE

5. Department of Paediatrics, Royal Children's Hospital, Melbourne, Australia

6. Department of Dermatology, King Edward Medical College, Nila Gumbad, Lahore, Pakistan

7. Department of Ophthalmology, Royal Victoria Hospital, Belfast, UK

8. Department of Paediatrics, St. James's University Hospital, Leeds, UK

9 Department of Paediatric Dermatology, Great Ormond Street Hospital for Children, London, UK

10. Department of Dermatology, Southern General Hospital, Glasgow, UK

*To whom correspondence should be addressed.
Tel: +44-1382-425618; Fax: +44-1382-425619; Email: wmclean@hgmp.mrc.ac.uk

ABSTRACT

Laryngo-onycho-cutaneous (LOC or Shabbir) syndrome (OMIM 245660) is an autosomal recessive epithelial disorder confined to the Punjabi Muslim population. The condition is characterised by cutaneous erosions, nail dystrophy and exuberant vascular granulation tissue in certain epithelia, especially conjunctiva and larynx. Genome-wide homozygosity mapping localised the gene to a 2 Mb region on chromosome 18q11.2 with a lod score of 19.8 at $\theta = 0$. This region includes the laminin α3 gene (*LAMA3*), in which loss-of-expression mutations cause the lethal skin blistering disorder Herlitz junctional epidermolysis bullosa. Detailed investigation showed that this gene possesses a further 38 exons (76 exons in total) spanning 318 kb of genomic DNA, and encodes 3 distinct proteins: designated laminin α3a, α3b1 and α3b2. The causative mutation in 15 families was a frameshift mutation 151insG predicting a stop codon 7 bp downstream in an exon that is specific to laminin α3a. This protein is secreted only by the basal keratinocytes of stratified epithelia, implying that LOC is caused by dysfunction of keratinocyte-mesenchymal communication. Surprisingly, the 151insG mutation does not result in nonsense-mediated mRNA decay due to rescue of the transcript by an alternative translation start site 6 exons downstream. The resultant N-terminal deletion of laminin α3a was confirmed by immunoprecipitation of secreted proteins from LOC keratinocytes. These studies show that the laminin α3a N-terminal domain is a key regulator of the granulation tissue response, with important implications not only in LOC but in a range of other clinical conditions associated with abnormal wound healing.

INTRODUCTION

Laryngo-onycho-cutaneous syndrome (LOC, OMIM 245660) is a chronic granulation tissue disorder seen in the Punjabi Muslim population. The disease was first characterised by Shabbir in 1986 (1), in 22 patients, all of whom shared significantly similar clinical features that had not been previously described. Eighteen of the 22 patients were children of consanguineous marriages between clinically normal individuals, strongly indicative of autosomal recessive inheritance. Some of the original families examined by Shabbir were studied here. All LOC families reported to date are of Punjabi descent (1-4) including all subjects in this report, suggesting a founder effect and perhaps an unusual defect that has not arisen in other populations. The term laryngeal and ocular granulation in children originating in the Indian subcontinent (LOGIC syndrome), has been suggested as an alternative name for the disorder (3).

Patients with LOC syndrome share common clinical features (**Fig. 1**). The onset is characterised by a hoarse cry soon after birth, although the physical appearance of these neonates is normal. Granulation tissue develops in the mucosal regions, nail bed and the larynx. Beginning in infancy, chronic skin ulcers and conjunctival lesions appear (1-4). Although eye involvement in LOC syndrome was not mentioned in the original description (1), ocular granulation tissue resembling a particularly aggressive pterygium has been reported in all subsequent patients described (2-4) and was a prominent feature in the patients studied here. In addition, there is failure of tooth enamel formation (2-4) and marked dental malformations (1) (**Fig. 1**). Many patients diagnosed with LOC syndrome do not live beyond childhood, the most common cause of premature death being acute or chronic respiratory obstruction with secondary pulmonary sepsis (2-4). However, patients who survive the early neonatal period often survive to adulthood (A.D. Irvine and C.S. Munro, personal observations) and symptoms of hoarseness and ulceration slowly improve with age (1). As granulation tissue accumulates in the larynx,

a permanent tracheostomy often becomes necessary to ensure a clear respiratory passageway. In addition, granulation tissue can spread to the epiglottis, trachea (3) and even the main bronchi (4). Furthermore, most of the older patients studied here are blind due to corneal pterygium formation.

Here, by genomewide homozygosity mapping in consanguineous families, we have localised the LOC gene to a 2 Mb interval on 18q11.2 and identified the causative mutation as an N-terminal deletion of the laminin α3a isoform.

MATERIALS AND METHODS

Homozygosity mapping

Patient and control lymphocyte DNA was extracted by standard techniques. Genome-wide homozygosity mapping was carried out essentially as described previously (5). Briefly, linkage analysis was initially carried out using four affected persons from consanguineous kindreds (Families 1-4) using microsatellite markers from the ABI PRISM Linkage Mapping Set, Version 2 (LMS2) and the ABI HD5 5 cM Mapping Set (PE Biosystems, Foster City, CA). Microsatellite PCR was performed according to the manufacturer's recommended protocol, using AmpliTaq Gold polymerase (PE Biosystems) in a 7.5 µl reaction volume, without multiplexing. Markers were sized on an ABI 377 automated DNA sequencer and data extracted and analysed using Genescan and Genotyper version 2.0 software, as previously described (6). When linkage was not detected using Families 1-4, the probands from Families 5 and 6 were analysed and an additional 60 fluorescent microsatellites were synthesised to fill gaps in the ABI panel (MWG Biotech AG, Ebersberg, Germany). Genetic linkage was initially scored "by eye" and where significant homozygosity was observed, additional families were analysed and two-point lod scores were calculated with MLINK algorithm of LINKAGE version 5.1.

The mutant allele frequency was assumed to be 0.00001 with 100% penetrance and marker allele frequencies were determined experimentally from a population of 50 unrelated unaffected Punjabi Muslims resident in the UK. Homozygosity was confirmed at the LOC locus in an additional family with documented consanguinity (Family 7). In Families 8-15, where the nature of the consanguinity was very distant or uncertain, calculations were done assuming that the parents were second cousins to simulate "fuzzy" inheritance (5). Recalculation assuming these parents to be more distantly related (third cousins) did not affect the resultant lod scores. The two intragenic microsatellite markers within the *LAMA3* gene, designated LAMA3GT1 and LAMA3GT2 were amplified using the PCR conditions above and the following primer pairs: LAMA3GT1.L (5' TTC TGG TCC TCT AAG AAT AC 3'), LAMA3GT1.R (5' CTT GAC TGC ATC TCC AAC C 3'); and LAMA3GT2.L (5' CAG GCA TTC TCT TAC CAG C 3'), LAMA3GT2.R (5' GGC TGA GAA GCA ATA AGT G 3'). The product sizes for the LAMA3GT1 and LAMA3GT2 markers were ~284 bp and ~192 bp, respectively.

Cell culture

Keratinocytes and dermal fibroblasts were cultured from skin biopsy material derived from an LOC patient (proband in Family 1) and a normal unrelated control, as previously described (7).

cDNA synthesis

mRNA was extracted from cultured cells or skin biopsy material using the Quick prep micro mRNA purification kit (Amersham-Pharmacia Biotech, St. Albans, UK) and reverse transcribed using oligo dT and AMV reverse transcriptase (Promega, Southampton, UK) for 1 hour at 45°C. For reverse transcription of long templates, samples were subjected to multiple rounds of reverse transcription, each time heating to

70°C for 10 min to break up RNA secondary structure and then cooling to 45°C with addition of further reverse transcriptase and further incubation at 45°C for 1 hour.

PCR

Unless otherwise stated, PCR was performed as follows. Approximately 50 ng of cDNA or 200 ng of genomic DNA was added to a premix containing PCR buffer (67 mM Tris-HCl pH 8.8, 16.6 mM $(NH_4)_2SO_4$, 1.5 mM $MgCl_2$, 0.17 mg/ml bovine serum albumin (Sigma, Poole, England), and 10 mM 2-mercaptoethanol), 10 nmol of each dNTP, 20 pmol of each primer in a total volume of 50 µl. After an initial denaturation at 95°C for 2 min, 1 unit of *Taq* polymerase (Promega, Crawley, UK) was added followed by 35 cycles of 95°C for 10 s, annealing temperature for 10 s, 72°C for 30 s, with a final incubation of 72°C for 5 min. For RT-PCR of *LAMA3* transcripts, a series of overlapping PCR fragments were generated using the primer pairs listed in **Table 1**. For direct amplification of exons, primer pairs were positioned within the introns flanking the exonic sequences (**Table 2**). The annealing temperatures for each primer pair are displayed in **Tables 1 & 2**. The PCR products were examined by 1% agarose gel electrophoresis, purified and directly sequenced as above. In some cases, particularly fragments involving the GC-rich 5' end of the gene, PCR was performed using Boehringer Long-Range buffer 1 (Roche Diagnostics, Mannheim, Germany) containing 1.75 mM $MgCl_2$. Reactions were subjected to a hot-start with 0.2 µl of Boehringer Long-Range DNA polymerase mix (Roche Diagnostics).

DNA sequencing and mutation detection

PCR products were purified for sequencing using QIA quick PCR purification kit (Qiagen, Crawley, UK). Purified fragments were directly sequenced with either the amplification primers or internal primers as appropriate using the Big-Dye Terminator chemistry on ABI 377 or ABI 3100 automated sequencers (Applied Biosystems, Foster

City, CA, USA). Mutation detection was carried out by manual comparison of patient sequences with normal control samples. Direct sequencing also was used to look for mutation 151insG in 50 normal unrelated British Caucasians and 50 unaffected unrelated British Punjabi Muslims resident in the UK with no family history of LOC syndrome. Mutation R943X (see Results) was confirmed in members of Family 15 by *Sal* I restriction enzyme digestion of exon 60 PCR products.

Electronic sequence analysis

DNA sequences were aligned, assembled and analysed using Geneworks version 2.5.1 (Oxford Molecular Systems, Oxford, UK). Promoter and transcriptional start site predictions were performed using the TSSG and TSSW algorithms, accessed via the Medical Research Council Human Gene Mapping Project website, (http://www.hgmp.mrc.ac.uk). BLAST analysis of DNA sequences was carried out via the National Center for Biotechnology Information website (http://www.ncbi.nlm.nih.gov). Recent assemblies of the human genome data were accessed through the University of California Santa Cruz website (http://genome.ucsc.edu). Additional microsatellite marker primer sequences and genetic mapping data were obtained from Généthon, Evry, France (http://www.genethon.fr) and The Center for Medical Genetics, Marshfield, WN, USA (http://research.marshfieldclinic.org).

Radioimmunoprecipitation assay

Keratinocytes from control and LOC patients were cultured as above in 24 well plates. Keratinocyte culture media was removed and cells were washed four times with PBS before the medium was replaced with 200µl methionine/cysteine deficient DMEM (Life Technologies, Paisley, UK) supplemented with 50µCi [^{35}S]-methionine (Amersham Biosciences UK Ltd, Buckinghamshire, UK) and incubated for 16 h at 37°C.

Radiolabelled conditioned medium was removed and micro-centrifuged for 5 min at 14,000 rpm to remove cellular debris before storage in aliquots at -20°C. Monoclonal antibody K140 against laminin β3 (1 μg) was added to 20 μl radiolabelled keratinocyte conditioned medium and incubated overnight at 4°C with rotation. 12 μg per sample of Protein G sepharose beads (Sigma) were swollen in radio-immunoprecipitation assay (RIPA) buffer (50 mM Tris-HCl, 150 mM NaCl, 0.5% NP-40) and incubated with samples for 3 h at 4°C. Beads with bound antibody-protein complexes were sedimented at 5000 rpm for 5 min and washed 3 times in RIPA buffer. Beads were resuspended in NuPAGE gel loading buffer plus reducing agent (InVitrogen, Groningen, The Netherlands) and heated to 70°C for 10 min before loading on 4-12% NuPAGE Bis-Tris gels (InVitrogen). Gels were fixed in 10% acetic acid: 50% methanol for 10 min and incubated in "Amplify" (Amersham Biosciences) for 30 min before drying and fluorography with Kodak Hyperfilm for 9 days at -80°C.

Immunohistochemistry

Part of a 4 mm punch biopsy from non-lesional thigh skin was embedded in OCT compound (Agar Scientific, Stansted, UK), snap frozen in liquid nitrogen-cooled isopentane and sectioned in a cryostat for subsequent indirect immunofluorescence microscopy, as described previously (8). Sections of normal skin were incubated with the same primary and secondary antibodies as controls. The primary antibodies included the following: GB3 (anti-laminin 5 trimer, SeraLabs, Loughborough, UK); SE144 (anti-laminin 5 γ2 chain, a gift from Gim Meneguzzi, Nice, France); BM2 (anti-laminin α3, a gift from Bob Burgeson, Boston, USA); K140 (anti-laminin β3, a gift from Peter Markinovich, Stanford, CA, USA); PKA1 (anti-laminin α3, gift from Peter Markinovich, Stanford, CA, USA); GOH3 (anti-α6 integrin, gift from Stephen Kennel, Oak Ridge, TN, USA); 450-9D (anti-β4 integrin, gift from Arnoud Sonnenberg, Amsterdam, The Netherlands); HD4-233 (anti-type XVII collagen, gift from Katsushi Owaribe, Nagoya,

Japan). Appropriate anti-species immunoglobulin secondary FITC antibody conjugates were obtained from Dako, Glostrup, Denmark.

Electron microscopy

Another part of the skin biopsy (above) was fixed in half-strength Karnovsky solution and osmium tetroxide, as detailed elsewhere (9). Ultrathin sections were stained with uranyl acetate and lead citrate and examined in a JEOL 100CX electron microscope.

RESULTS

Clinical details

All living patients and their families were seen and examined by one or more of the authors (ADI, CSM, RP or TJ). Families from a Pakistani Punjabi background were seen in Scotland, England, Northern Ireland, France and in Pakistan (Lahore and the surrounding Punjab region). Medical records for living patients and possibly affected deceased relatives were examined where available in the local health care setting in conjunction with local health professionals. Due to the range of health care institutions that the subjects had attended (basic rural health care in some, tertiary referral hospital for others) there was a wide variation in the degree of clinical investigations and medical interventions performed. To ensure a consistent approach, ascertainment of affected phenotype for the purposes of this study was based on clinical history and physical examination and not on the basis of laboratory investigations. After review of the few clinical papers published to date (1-4) and discussion with the original authors, subjects were deemed to be affected with LOC if they fulfilled the following clinical diagnostic criteria: (1) hoarse cry in first few weeks of life or evidence of laryngeal granulation tissue, scarring or stenosis in the first few years of life; (2) nail dystrophy; (3) ocular involvement including aggressive conjunctival pannus formation; (4) dental anomalies (hypodontia, poor enamel formation, excessive caries); (5) slow-healing cutaneous erosions; (6) absence of a history of skin fragility or blistering at any stage. All subjects deemed affected in the study filled all of these criteria. The cardinal features of LOC syndrome are illustrated in **Fig. 1**. Patient DNA and tissue samples were obtained after

informed consent with the approval of the relevant local Ethics Committees.

Genetic linkage analysis

To search for the LOC gene, we carried out genomewide homozygosity mapping using the ABI HD5 linkage mapping panel, consisting of 800 fluorescent microsatellite markers, as described previously (5). Affected individuals were genotyped from six apparently unrelated Punjabi families (**Fig. 2a**). Five of these kindreds are UK citizens of Punjabi ancestry (Families 1-4 & 6) and the other family resides in the Lahore region of Pakistan (Family 5). Initial screening identified potential loci on chromosomes 5q in the vicinity of D5S400 and 16q, in the region of D16S3061. However, these loci were suspected as false linkage due to lack of shared haplotypes between the families. Analysis of additional LOC families completely excluded these loci (data not shown). No other suspect loci were identified from the initial screen. In case the locus had been missed, the larger gaps in the HD5 panel were filled by synthesis of an additional 60 microsatellites. One of these additional markers, D18S869 showed homozygosity for the same allele (195 bp) in all but three of our 15 LOC families, consistent with the anticipated founder effect (**Fig. 2b**). Further genotyping was carried out with an additional nine closely spaced microsatellites in the vicinity of D18S869. This revealed an area of shared haplotype for three markers, LAMA3GT1, LAMA3GT2 (see below) and D18S1101 in 17 individuals from 14 LOC families (**Fig. 2b**). One family remained unlinked (Family 15), however, in this case, one parent carried the linked haplotype (**Fig. 2b**). There was no evidence of consanguinity in Family 15 and therefore, it was assumed that the affected individual in this case might represent a compound heterozygote. All parents of affected individuals in Families 1-14 were heterozygous for the linked haplotype and no unaffected siblings of LOC patients were homozygous for this haplotype. For the kindreds where details of consanguinity were known (Families 1-7), markers within the region of shared haplotype gave a highly significant two-point lod

score of 9.6 at $\theta = 0$. The combined two-point lod score for all kindreds showing linkage (Families 1-14) was 19.8 at $\theta = 0$ for the three markers within the region of shared haplotype.

The limits of the LOC locus were defined by visible recombinations seen in Families 2, 7 and 12 (individuals 2-1, 7-1 and 12-2; **Fig. 2b**) with markers D18S869 (centromeric) and D18S480 (telomeric). This gave a critical interval of approximately 2 Mb of genomic DNA (UCSC Genome Map). A total of 12 known and strongly predicted genes were located in this interval. Of these, *LAMA3*, located centrally, was considered by far the most likely candidate gene on the basis of its biological functions. Laminin $\alpha 3$ is one of the three polypeptides comprising laminin 5, the major cutaneous basement membrane laminin with a critical function in adhesion of the epidermis to the dermis. Loss-of-expression mutations in *LAMA3* cause the skin blistering disorder Herlitz junctional epidermolysis bullosa (H-JEB) (10-12). In addition to mediating cell-substratum adhesion, laminins in general and laminin 5 in particular have important additional functions in the control of cell migration and behaviour (13, 14). Therefore, since the main phenotype in LOC is uncontrolled production of granulation tissue in the skin and other epithelial tissues, *LAMA3* was considered a prime candidate. Two microsatellites within introns 12 and 41 of the extended *LAMA3* gene (described in detail below), designated LAMA3GT1 and LAMA3GT2, respectively, were found to be highly polymorphic in the Punjabi Muslim population. Importantly, the relevant haplotype for these two markers (alleles 290 and 195, respectively) was shared by all LOC affected individuals studied (**Fig. 2b**), including one copy carried by the presumptive compound heterozygote Family 15. Therefore, the *LAMA3* gene falls within the region of shared haplotype within the LOC locus.

LAMA3 gene structure and alternate splicing

The *LAMA3* gene was initially reported as having 38 exons encoding the laminin α3a polypeptide (15). However, partial cDNAs have been reported encoding a longer alternate transcript which encodes the larger laminin α3b polypeptide, whose functions and protein interactions are less well understood (15, 16). Since recessive loss-of-function mutations in *LAMA3A* had already been demonstrated in the severe/lethal skin blistering disorder H-JEB, we initially focused on *LAMA3B*. Analysis of the human genome sequence with reference to the reported laminin α3b cDNAs and ESTs revealed an additional 38 exons upstream of the existing 38 *LAMA3A* exons, giving a total of 76 exons spanning 318 kb of genomic DNA. The full gene structure and transcripts thereof are shown in **Fig. 3**. Exons 1-38 plus 40-76 encode the longer *LAMA3B* transcript (i.e. exon 39 is skipped in the *LAMA3B* isoform). In addition, RT-PCR performed on cDNA extracted from normal control keratinocytes revealed that about 20% of the *LAMA3B* mRNA also lacks exon 10. We propose that the longer *LAMA3B* isoform should be designated *LAMA3B1* (encoding laminin α3b1) and that the shorter version lacking exon 10 be designated *LAMA3B2* (encoding laminin α3b2). The predicted laminin α3b1 polypeptide consists of 3333 amino acids and has a calculated molecular weight of 366.3 kDa. The shorter laminin α3b2 polypeptide is comprised of 3289 amino acids and has a calculated molecular weight of 361.4 kDa. Promoter sequences immediately upstream of exon 1 (B-isoforms) were strongly predicted by both the TSSG and TSSW algorithms (17). The transcriptional start site of the B isoforms was mapped by RT-PCR (data not shown) and the entire *LAMA3B1* and *LAMA3B2* cDNAs were amplified in a series of overlapping RT-PCR fragments and fully sequenced. Primers used for RT-PCR are listed in **Table 1**.

The *LAMA3A* transcript starts with exon 39, which includes the initiation codon and 5' UTR of the *LAMA3A* transcript, and includes exons 39-78 of the *LAMA3* gene. However, the *LAMA3A* 5' UTR derived from the human genome sequence (UCSC Browser) was

found to have slight differences from the published mRNA sequence and contained an additional in-frame ATG codon (**Fig. 4**). The sequences surrounding the new ATG conform better to the Kozak consensus sequence than the previously proposed initiation codon (15). This sequence was verified by sequencing of both genomic and RT-PCR fragments, and the likely transcriptional start site predicted by both the TSSG and TSSW algorithms was determined by RT-PCR of keratinocyte mRNA using a series of primers across the region (**Fig. 4**). The *LAMA3A* promoter was strongly predicted by both the TSSG and TSSW algorithms to be within intron 38, immediately upstream of exon 39. The entire *LAMA3A* cDNA was amplified in a series of overlapping fragments and was fully sequenced. Primers used for RT-PCR are listed in **Table 1**. The predicted laminin α3a polypeptide consists of 1724 amino acids and has a calculated molecular weight of 190.3 kDa. By RT-PCR, the A-isoform was found to be both specifically and highly expressed by epidermal keratinocytes but not by dermal fibroblasts, whereas the two B-isoforms were expressed by both these cell types (data not shown). Relative expression was not assessed in other tissues. The Genbank accession numbers for the *LAMA3* transcripts determined here are as follows: AY327114 (*LAMA3A*); AY327115 (*LAMA3B1*) and AY327116 (*LAMA3B2*).

Isoform-specific LAMA3 mutation in LOC

PCR conditions were developed to amplify the individual exons of the *LAMA3* gene using intronic primers to facilitate mutation detection based on genomic DNA (primers detailed in **Table 2**). All 76 exons were screened for mutations in LOC affected individuals by direct sequencing of genomic PCR products, with comparison to normal unrelated controls. In LOC patients from Families 1-14, a homozygous 1 bp insertion mutation was detected in exon 39, the exon found exclusively in the keratinocyte-specific *LAMA3A* transcript encoding the laminin α3a polypeptide (**Fig. 5**). The mutation was designated 151insG, numbering from the initiating ATG of our revised *LAMA3A*

sequence (**Fig. 4**; Genbank accession number AY327114) and leads to a premature termination codon (PTC) 7 bp after the insertion, within this first *LAMA3A* exon. Numbering from the previously reported mRNA sequences (Genbank accession numbers NM_000227 and X77598), this mutation would be designated 118insG. All parents in Families 1-14 were heterozygous carriers of the mutation (**Fig. 5**). Thus, individuals with LOC are homozygous for a frameshift mutation leading to a PTC within the only exon specific to the *LAMA3A* isoform. This mutation should have no effect on expression of the *LAMA3B* isoforms and therefore our initial hypothesis was that LOC is caused by a specific, differential loss of laminin α3a expression. In contrast, all the *LAMA3* mutations reported in H-JEB patients are PTC mutations in exons that are common to both *LAMA3A* and *LAMA3B* transcripts (10, 12). Therefore, we hypothesised that loss of both laminin α3a and α3b expression might cause H-JEB, whereas, loss of α3a alone would cause LOC.

The father in Family 15, who carried the shared LOC haplotype (**Fig. 2b**), was also found to carry the ancestral 151insG mutation, which he had passed on to his affected son but this was not detected in the mother's DNA. All other exons of the *LAMA3* gene were analysed in the Family 15 proband and his parents. Both the proband and his mother were found to be heterozygous for nonsense mutation R943X (DNA change 2827C>T) in exon 60, the 22nd exon of the *LAMA3A* transcript (**Fig. 6**). This mutation would be numbered R932X in the previously reported sequence. The mutation ablates a *Sal* I restriction enzyme site which was used to confirm the mutation in the proband and his mother and exclude it from his father (**Fig. 6**). Thus, the proband in Family 15 is a compound heterozygote for mutations 151insG and R943X in *LAMA3A*. This individual would be predicted to lack expression of laminin α3a but would express 50% of the normal amount of laminin α3b, again consistent with the hypothesis that LOC is caused by loss of laminin α3a alone.

By direct DNA sequencing, the incidence of the common LOC mutation was investigated in 50 normal unrelated British Punjabi Muslims with no family history of LOC syndrome as well as 50 normal unrelated British Caucasians. The mutation was not detected in the British Caucasian control population. However, one Punjabi control was found to be heterozygous for the 151insG mutation, indicating that this mutant *LAMA3A* allele may be fairly common in the Punjabi population.

Rescue of the LOC mutant transcript

To see if the 151insG mutation would lead to nonsense-mediated mRNA, we obtained a skin biopsy from a heterozygous carrier of the LOC mutation;mRNA was extracted and subjected to RT-PCR using a forward primer within exon 39 and reverse primer in exon 42, so that only the *LAMA3A* transcript would be amplified. mRNA was pre-treated with RNAse-free DNAse I and phenol-chloroform extracted to safeguard against genomic DNA contamination. Direct sequencing of this RT-PCR product (**Fig. 7a**) was compared to a genomic exon 39 fragment from the same individual sequenced with the same primer (**Fig. 7b**). Surprisingly, the sequence traces obtained from genomic DNA and cDNA were essentially identical, with the overlapping sequence traces due to the insertion clearly visible in both samples and present at very similar levels. Therefore, this demonstrates that the 151insG mutation does not lead to appreciable nonsense-mediated decay of the *LAMA3A* transcript.

Close examination of the *LAMA3A* mRNA sequence revealed that the wild-type 5' UTR does not contain any in-frame stop codons (**Fig. 4**) whereas many 5' UTRs do, especially longer ones (18, 19). We hypothesised that the translation machinery may regard this premature stop codon near the start of the mRNA as a natural feature of the 5' UTR and therefore translation might occur from another ATG downstream if one existed within the

context of a suitable Kozak consensus motif, which is required for efficient translation. The next ATG codon downstream of the frameshift occurs in exon 45 (methionine 218 in the revised protein sequence), however, this codon is a very poor fit for the Kozak consensus (**Fig. 7c**). In contrast, the next ATG, also in exon 45 (methionine 227) is a perfect fit for the Kozak sequence (18), in fact conforming to the consensus much better than the natural initiation codon of the *LAMA3A* transcript (**Fig. 7c**). Thus, it seemed plausible that protein translation would initiate from this codon leading to a truncated laminin α3a polypeptide lacking the first 226 amino acids. To look for this truncated protein and to see if it would be assembled into trimeric laminin 5 and secreted from keratinocytes, we performed immunoprecipitation of radiolabelled secreted proteins from control and LOC keratinocytes using an antibody specific for the C-terminus of laminin β3 (20, 21). This analysis revealed that indeed a truncated laminin α3a is synthesised, assembled and secreted by LOC keratinocytes (**Fig. 8**). The reduction in size of the truncated protein compared to wild-type laminin α3a was consistent with loss of 226 amino acids (~24 kDa). Thus, the LOC mutant transcript is rescued by a novel mechanism leading to expression of an N-terminally truncated protein. We propose the term "delayed initiation codon" for this novel class of mutation.

Subtle morphological changes in LOC skin

Using frozen skin biopsy material from an LOC patient (proband in Family 1, homozygous for the 151insG mutation) and a normal unrelated control, we performed immunofluorescence staining with a variety of antibodies against all three α3, β3 and γ2 chains of the laminin 5 trimer and other components of the cutaneous basement membrane zone. Representative results are shown in **Fig. 9**. Essentially, all antigens examined, including laminin α3, were present in normal amounts and were distributed normally. The laminin α3 antibodies used are not able to distinguish laminin α3a and α3b isoforms, nevertheless, there was no evidence of a 50% reduction in staining

intensity that one might expect if the α3a isoform was absent. Importantly, normal staining was obtained in LOC skin with monoclonal antibody GB3, which detects trimeric laminin 5 (22), confirming the assembly and secretion of this protein complex.

The ultrastructure of the dermal-epidermal junction (DEJ) was generally normal, but there were some subtle qualitative changes (**Fig. 10**). The number of hemidesmosomes and anchoring fibrils, appeared to be normal. However, some of the hemidesmosome plaques were small and lacked normal sub-basal dense plates. These diminutive cell-stromal junctions were associated with reduced numbers of anchoring filaments and focal widening of the lamina lucida, the site of laminin 5 localisation within the DEJ. There were no overt splits in the lamina lucida, as would be expected in the junctional forms of epidermolysis bullosa, such as H-JEB.

DISCUSSION

LOC syndrome is a rare recessive disorder thus far only described in the Punjabi Muslim population (1-4, 23). The disease is characterised by chronic production of vascular granulation tissue which invades and disrupts specific epithelial tissues, notably the conjunctiva and anterior corneal epithelium (4, 23), as well as the respiratory mucosae. Here, by genome-wide homozygosity mapping we localised the gene causing LOC syndrome to a small interval on human chromosome 18q. The causative mutation in all but one family was found to be homozygosity for a novel class of mutation in the laminin α3 gene (*LAMA3*). The remaining case was a compound heterozygote for this mutation and a complementary null-allele. The ancestral genetic defect was a delayed initiation codon mutation in exon 39 of *LAMA3*, designated 151insG. Exon 39 is the first exon of the *LAMA3A* transcript, which encodes the laminin α3a polypeptide, a component of the laminin 5 heterotrimer, a basement membrane laminin specifically secreted by basal

keratinocytes in the skin and other stratified epithelia including airway and ocular epithelia (22, 24). Furthermore, the mutated exon is the only one specific to laminin α3a and is spliced out of laminin α3b1 and α3b2 described here, whose functions are currently unknown. Unexpectedly, we found that this frameshift mutation does not lead to appreciable nonsense-mediated decay of the *LAMA3A* mRNA. The mutant transcript escapes accelerated degradation by utilising an alternative initiation codon downstream (in exon 45) which occurs in the context of a particularly good Kozak sequence (18). Effectively, this leads to an N-terminal deletion of 226 amino acids from the laminin α3a isoform. Here, the mutant polypeptide is synthesised, assembled and secreted efficiently by keratinocytes from LOC patients. In general, PTC mutations located towards the 5' end of mRNA species would be expected to give near-complete absence of protein expression (25). However, here we show that in certain cases at least, PTCs located at the extreme 5'end may escape nonsense-mediated decay if a suitable alternative initiation codon exists within the message, even at a considerable distance downstream. These observations have important implications for predicting the effects of future 5' frameshift or nonsense mutations.

Laminin 5 is a heterotrimer composed of α3a, β3 and γ2 chains (22, 26-28). It has been shown that these molecules must undergo trimerisation in order to be secreted by keratinocytes (29). We showed here by immunoprecipitation that a mutant form of laminin α3a lacking the first 226 amino acids (~24 kDa) is able to assemble with laminin β3 and γ2 to form laminin 5 trimers that are capable of being secreted by cultured keratinocytes. This *in vitro* result is borne out by the fact that immunohistochemical analysis of LOC patient skin showed no obvious qualitative or quantitative aberrations with antibodies against all three laminin 5 polypeptides. Importantly, staining for antibody GB3 was normal in LOC skin. The GB3 epitope is conformation-dependant and is completely lost in cases of H-JEB when any of the three laminin 5 chains are

absent (30, 31) and therefore positive staining for GB3 provides further evidence for laminin 5 trimerisation and secretion. Ultrastructural analysis was again unremarkable. In particular, there was no overt separation of the skin, consistent with the relatively mild erosive skin phenotype in LOC, rather than the extremely fragile skin as is the case in H-JEB (12, 32). Furthermore, anchoring filaments, which are composed largely of laminin 5 and generally absent in HJEB , were clearly visible in the skin of an LOC patient. From this, we conclude that N-terminally truncated laminin α3a is both assembly-competent and capable of making anchoring filaments extracellularly in the cutaneous basement membrane zone. Only very subtle ultrastructural changes were seen, such as focal widening of the lamina lucida, demonstrating that the truncated protein is largely able to perform its primary function in mediating keratinocyte-stromal adhesion. In contrast, a genetic mutation that reduces the levels of laminin 5 expression has been shown to lead to a skin blistering phenotype (33). It should be noted that excessive granulation tissue production is in fact seen in HJEB and non-lethal forms of JEB (34, 35), particularly affecting facial skin as is the case in LOC (**Fig. 1**). Thus, complete or partial ablation of the entire laminin 5 trimer also leads to exuberant granulation tissue as would be expected from our results. However, the severe or lethal skin fragility in JEB patients tends to mask this aspect of the phenotype.

The main phenotype in LOC syndrome is chronic production of vascular granulation tissue often with activation and invasive migration of fibroblasts resulting in neovascularisation. However, the defective molecule, laminin α3a, is synthesised only by basal keratinocytes of stratified epithelia, implying that LOC is a disorder of keratinocyte-mesenchymal communication. Since the structural consequences of this laminin α3a defect are very subtle, it is likely that the aberrant mesenchymal cell behaviour is due to a lost keratinocyte signalling function that resides in the truncated N-terminal domain of laminin α3a. Thus, identification of the LOC defect may shed some

light on how the granulation tissue response is normally controlled. It has been shown previously that the C-terminus of laminin α3a interacts with the extracellular domains of the integrin α6β4 through a series of G-domain repeats (36, 37). These C-terminal repeats can be proteolytically cleaved (38, 39) in a manner that affects cell behaviour and migration during wound healing (36). Thus, in the basement membrane of skin and other stratified epithelia, the laminin 5 trimer exists in an inverted cruciform configuration with the N-terminus of laminin α3a orientated towards the mesenchyme (36). It is therefore possible that the N-terminal domain normally acts as a signal to the underlying mesenchyme that the basement membrane is intact. When a stratified epithelium is damaged such that the basement membrane is breached, cytokines and other soluble factors derived from the epithelium will activate a mesenchymal wound healing response in addition to initiating epithelial repair activity. When the wound is closed and re-epithelialised, the basement membrane is re-established and at this stage, the laminin α3a N-terminal domain may act as a "brake" to deactivate fibroblasts and/or endothelial cells to terminate the mesenchymal wound healing response. In this model, the negative signal is absent in LOC syndrome, and so the granulation tissue response, once activated by physical trauma in certain delicate epithelia, such as the mucosae or ocular epithelia, cannot be deactivated and continues in an uncontrolled manner. Proteolytic cleavage of the C-terminal G-domains of laminin α3a has been shown to be important in the control of keratinocyte growth and migration (13, 37). Furthermore, synthetic peptides analogous to sequences in the N-terminal domains of a number of classical full-length laminin alpha chains, including equivalent sequences specific to the laminin α3b chains described here, have been shown to modulate endothelial cell attachment, migration and growth (40). However, similar investigations of the specific N-terminus of laminin α3a have not yet been performed. Here, this domain is shown to be important in control of mesenchymal cell growth and migration. Thus, the cutaneous basement membrane, which has functions in mediating epithelial-stromal adhesion, can also be regarded as

having a double-sided signalling function mediated by the N- and C-termini of laminin α3a.

The critical interactions through which the N-terminus of laminin α3a might mediate mesenchymal cell signalling are as yet unknown. Possibilities include a direct interaction with a cell surface receptor expressed by mesenchymal cells or alternatively the domain might interact with other extracellular matrix molecules and the resultant macromolecular complex may influence cell behaviour. Granulation tissue is a major clinical problem, not only in LOC syndrome but in a range of much more common conditions such as rheumatoid arthritis, chronic venous leg ulcers, transplant surgery and others. A fuller understanding of the role of laminin α3a in this sometimes undesirable biological process might lead to the identification of novel targets for therapeutic intervention.

ACKNOWLEDGEMENTS

This manuscript is dedicated to the memory of our co-author Professor Syed Ghulam Shabbir, who sadly passed away in 2002. The authors would like to express their thanks to the patients, their families and healthy volunteers from the British Punjabi community without whom this research would not have been possible. Thanks also to Andrew J. Cassidy, DNA Analysis Facility, Human Genetics Unit, Ninewells Medical School, for DNA sequencing and genotyping support services. This work was supported by grants from The Dystrophic Epidermolysis Bullosa Research Association (to WHIM and JAM); Action Research (JAM); The Wellcome Trust (Senior Research Fellowship in Basic Biomedical Sciences to WHIM supporting WHIM and FJDS and a Prize PhD Studentship supporting KJH); and the Hasham M. Jamil Trust (WHIM and ADI).

REFERENCES

1. Shabbir, G., Hassan, M., and Kazmi, A. (1986) Laryngo-onycho-cutaneous syndrome: a study of 22 cases. *Biomedica*., **2**, 15-25.

2. Phillips, R. J., Atherton, D. J., Gibbs, M. L., Strobel, S., and Lake, B. D. (1994) Laryngo-onycho-cutaneous syndrome: an inherited epithelial defect. *Arch. Dis. Child.*, **70**, 319-326.

3. Ainsworth, J. R., Spencer, A. F., Dudgeon, J., Geddes, N. K., and Lee, W. R. (1991) Laryngeal and ocular granulation tissue formation in two Punjabi children: LOGIC syndrome. *Eye*., **5**, 717-722.

4. Ainsworth, J. R., Shabbir, G., Spencer, A. F., and Cockburn, F. (1992) Multisystem disorder of Punjabi children exhibiting spontaneous dermal and submucosal granulation tissue formation: LOGIC syndrome. *Clin. Dysmorph.*, **1**, 3-14.

5. Hamada, T., McLean, W. H. I., Ramsay, M., Ashton, G. H., Nanda, A., Jenkins, T., Edelstein, I., South, A. P., Bleck, O., Wessagowit, V., Mallipeddi, R., Orchard, G. E., Wan, H., Dopping-Hepenstal, P. J., Mellerio, J. E., Whittock, N. V., Munro, C. S., van Steensel, M. A., Steijlen, P. M., Ni, J., Zhang, L., Hashimoto, T., Eady, R. A. J., and McGrath, J. A. (2002) Lipoid proteinosis maps to 1q21 and is caused by mutations in the extracellular matrix protein 1 gene (ECM1). *Hum Mol Genet*., **11**, 833-840.

6. van Steensel, M., Smith, F. J., Steijlen, P. M., Kluijt, I., Stevens, H. P., Messenger, A., Kremer, H., Dunnill, M. G., Kennedy, C., Munro, C. S., Doherty, V. R., McGrath, J. A., Covello, S. P., Coleman, C. M., Uitto, J., and McLean, W. H. (1999) The gene for hypotrichosis of Marie Unna maps between D8S258 and D8S298: exclusion of the hr gene by cDNA and genomic sequencing. *Am J Hum Genet*., **65**, 413-419.

7. Leigh, I. M., Lane, E. B., and Watt, F. M. 1994. The Keratinocyte Handbook. Cambridge University Press, Cambridge.

8. McGrath, J. A., Hoeger, P. H., Christiano, A. M., McMillan, J. R., Mellerio, J. E., Ashton, G. H., Dopping-Hepenstal, P. J., Lake, B. D., Leigh, I. M., Harper, J. I., and Eady, R. A. (1999) Skin fragility and hypohidrotic ectodermal dysplasia resulting from ablation of plakophilin 1. *Br J Dermatol*., **140**, 297-307.

9. Eady, R. A. J. (1985) Transmission electron microscopy. *In* Skerrow, D. and Skerrow, C. J., (eds.), *Methods in Skin Research*. John Wiley & Sons, Chichester, pp. 1-36.

10. Uitto, J., Pulkkinen, L., and McLean, W. H. I. (1997) Epidermolysis bullosa: A spectrum of clinical phenotypes explained by molecular heterogeneity. *Mol. Med. Today*., **3**, 457-465.

11. Fine, J. D., Eady, R. A., Bauer, E. A., Briggaman, R. A., Bruckner-Tuderman, L., Christiano, A., Heagerty, A., Hintner, H., Jonkman, M. F., McGrath, J., McGuire, J., Moshell, A., Shimizu, H., Tadini, G., and Uitto, J. (2000) Revised classification system for inherited epidermolysis bullosa: Report of the Second International Consensus Meeting on diagnosis and classification of epidermolysis bullosa. *J Am Acad Dermatol*., **42**, 1051-1066.

12. Uitto, J., Pulkkinen, L., and Ringpfeil, F. (2002) Progress in molecular genetics of heritable skin diseases: the paradigms of epidermolysis bullosa and pseudoxanthoma elasticum. *J Investig Dermatol Symp Proc*., **7**, 6-16.

13. O'Toole, E. A. (2001) Extracellular matrix and keratinocyte migration. *Clin Exp Dermatol*., **26**, 525-530.

14. Lohi, J. (2001) Laminin-5 in the progression of carcinomas. *Int J Cancer*., **94**, 763-

767.

15. Vidal, F., Baudoin, C., Miquel, C., Galliano, M. F., Christiano, A. M., Uitto, J., Ortonne, J. P., and Meneguzzi, G. (1995) Cloning of the laminin alpha-3 chain gene (lama3) and identification of a homozygous deletion in a patient with herlitz junctional epidermolysis-bullosa. *Genomics*., **30**, 273-280.

16. Ferrigno, O., Virolle, T., Galliano, M. F., Chauvin, N., Ortonne, J. P., Meneguzzi, G., and Aberdam, D. (1997) Murine laminin alpha3A and alpha3B isoform chains are generated by usage of two promoters and alternative splicing. *J Biol Chem*., **272**, 20502-20507.

17. Solovyev, V., and Salamov, A. (1997) The Gene-Finder computer tools for analysis of human and model organisms genome sequences. *Proc Int Conf Intell Syst Mol Biol*., **5**, 294-302.

18. Lewin, B. 2000. Genes VII. Oxford University Press, Oxford.

19. Cooper, D. N., and Krawczak, M. 1993. Human Gene Mutation. BIOS Scientific Publishers Ltd., Oxford.

20. Marinkovich, M. P., Verrando, P., Keene, D. R., Meneguzzi, G., Lunstrum, G. P., Ortonne, J. P., and Burgeson, R. E. (1993) Basement membrane proteins kalinin and nicein are structurally and immunologically identical. *Lab Invest*., **69**, 295-299.

21. Meneguzzi, G., Marinkovich, M. P., Aberdam, D., Pisani, A., Burgeson, R., and Ortonne, J. P. (1992) Kalinin is abnormally expressed in epithelial basement membranes of Herlitz's junctional epidermolysis bullosa patients. *Exp Dermatol*., **1**, 221-229.

22. Verrando, P., Hsi, B.-L., Yeh, C.-J., Pisani, A., Serieys, N., and Ortonne, J.-P. (1987) Monoclonal antibody GB3, a new probe for the study of human basement membranes

and hemidesmosomes. *Exp Cell Res*., **170**, 116-128.

23. Moore, J. E., Dua, H. S., Page, A. B., Irvine, A. D., and Archer, D. B. (2001) Ocular surface reconstruction in LOGIC syndrome by amniotic membrane transplantation. *Cornea*., **20**, 753-756.

24. Marinkovich, M. P., Keene, D. R., Rimberg, C. S., and Burgeson, R. E. (1993) Cellular origin of the dermal-epidermal basement membrane. *Dev Dyn*., **197**, 255-267.

25. Cooper, D. N. (1993) Human gene mutation affecting RNA processing and translation. *Ann Med*., **25**, 11-17.

26. Carter, W. G., Ryan, M. C., and Gahr, P. J. (1991) Epiligrin, a new cell adhesion ligand for integrin alpha 3 beta 1 in epithelial basement membranes. *Cell*., **65**, 599-610.

27. Rousselle, P., Lunstrum, G. P., Keene, D. R., and Burgeson, R. E. (1991) Kalinin: an epithelium-specific basement membrane adhesion molecule that is a component of anchoring filaments. *J Cell Biol*., **114**, 567-576.

28. Burgeson, R. E., Chiquet, M., Deutzmann, R., Ekblom, P., Engel, J., Kleinman, H., Martin, G. R., Meneguzzi, G., Paulsson, M., Sanes, J., and et al. (1994) A new nomenclature for the laminins. *Matrix Biol*., **14**, 209-211.

29. Cheng, Y. S., Champliaud, M. F., Burgeson, R. E., Marinkovich, M. P., and Yurchenco, P. D. (1997) Self-assembly of laminin isoforms. *J Biol Chem*., **272**, 31525-31532.

30. Shimizu, H., Schofield, O. M., and Eady, R. A. (1991) [Prenatal diagnosis of lethal junctional epidermolysis bullosa by fetal skin biopsy]. *Nippon Hifuka Gakkai Zasshi*., **101**, 539-545.

31. Verrando, P., Schofield, O., Ishida-Yamamoto, A., Aberdam, D., Partouche, O., Eady, R. A., and Ortonne, J. P. (1993) Nicein (BM-600) in junctional epidermolysis bullosa: polyclonal antibodies provide new clues for pathogenic role. *J Invest Dermatol*., **101**, 738-743.

32. Christiano, A. M., and Uitto, J. (1996) Molecular complexity of the cutaneous basement membrane zone. Revelations from the paradigms of epidermolysis bullosa. *Exp Dermatol*., **5**, 1-11.

33. Spirito, F., Chavanas, S., Prost-Squarcioni, C., Pulkkinen, L., Fraitag, S., Bodemer, C., Ortonne, J. P., and Meneguzzi, G. (2001) Reduced expression of the epithelial adhesion ligand laminin 5 in the skin causes intradermal tissue separation. *J Biol Chem*., **276**, 18828-18835.

34. Lim, K.K., Su, W.P., McEvoy, M.T. and Pittelkow, M.R. (1996) Generalized gravis junctional epidermolysis bullosa: case report, laboratory evaluation, and review of recent advances. *Mayo Clin Proc,* **71**, 863-8.

35. Carter, D.M., Lin, A.N., Varghese, M.C., Caldwell, D., Pratt, L.A. and Eisinger, M. (1987) Treatment of junctional epidermolysis bullosa with epidermal autografts. *J Am Acad Dermatol,* **17**, 246-50.

36. Goldfinger, L. E., Hopkinson, S. B., deHart, G. W., Collawn, S., Couchman, J. R., and Jones, J. C. (1999) The alpha3 laminin subunit, alpha6beta4 and alpha3beta1 integrin coordinately regulate wound healing in cultured epithelial cells and in the skin. *J Cell Sci*., **112**, 2615-2629.

37. Hirosaki, T., Mizushima, H., Tsubota, Y., Moriyama, K., and Miyazaki, K. (2000)

Structural requirement of carboxyl-terminal globular domains of laminin alpha 3 chain for promotion of rapid cell adhesion and migration by laminin-5. *J Biol Chem*., **275**, 22495-22502.

38. Tsubota, Y., Mizushima, H., Hirosaki, T., Higashi, S., Yasumitsu, H., and Miyazaki, K. (2000) Isolation and activity of proteolytic fragment of laminin-5 alpha3 chain. *Biochem Biophys Res Commun*., **278**, 614-620.

39. Amano, S., Scott, I. C., Takahara, K., Koch, M., Champliaud, M. F., Gerecke, D. R., Keene, D. R., Hudson, D. L., Nishiyama, T., Lee, S., Greenspan, D. S., and Burgeson, R. E. (2000) Bone morphogenetic protein 1 is an extracellular processing enzyme of the laminin 5 gamma 2 chain. *J Biol Chem*., **275**, 22728-22735.

40. Nomizu, M., Yokoyama, F., Suzuki, N., Okazaki, I., Nishi, N., Ponce, M. L., Kleinman, H. K., Yamamoto, Y., Nakagawa, S., and Mayumi, T. (2001) Identification of homologous biologically active sites on the N-terminal domain of laminin alpha chains. *Biochemistry*., **40**, 15310-15317.

FIGURE LEGENDS

Figure 1

Clinical features of LOC syndrome in patients from Families 2 & 3.

a. Proband in Family 3, showing cutaneous erosions on the face, which are slow to heal. Healed lesions often leave behind atrophic, pigmented scars as seen on the right cheek of this patient

b. Nail dystrophy is common in LOC; in infants erosions are often seen but older patients develop a thickened hyperkeratotic appearance, seen here in right great toe of the proband from Family 2.

c. Ocular granulation tissue with lateral symblepharon formation in the proband from Family 2. This patient in his 20's, is blind due to almost complete closure of the eyelids and deep corneal scarring secondary to the invasive fibrovascular growth.

d. Hypoplastic enamel and subsequent carious teeth are common findings in LOC. (proband of Family 2).

Figure 2

a. Pedigrees of consanguineous LOC Families 1-6, used for genome-wide homozygosity mapping. Arrows indicate probands and numbers refer to individual probands whose haplotypes are shown in (b), below. Asterisks show individuals from whom DNA was available for study.

b. Haplotypes of affected LOC individuals for microsatellite markers in the vicinity of the LOC locus. Numbers above haplotypes refer to individual LOC patients and are in

the format Family-Patient number. Boxes indicate areas of homozygosity-by-descent.

Figure 3

a. Schematic diagram (to scale) showing the genomic organisation of the 76 exons of the *LAMA3* gene, which spans ~318 kb on chromosome 18q. Exons involved in transcription initiation and/or alternate splicing are indicated by arrows.

b. Transcripts identified from the *LAMA3* gene (spliced exons to scale). These transcripts encode three laminin α3 polypeptides: α3a, α3b1 and α3b2. The predicted laminin α3a polypeptide consists of 1724 amino acids and has a calculated molecular weight of 190.3 kDa. The predicted laminin α3b1 protein consists of 3333 amino acids and has a calculated molecular weight of 366.3 kDa. The shorter laminin α3b2 polypeptide is comprised of 3289 amino acids and has a calculated molecular weight of 361.4 kDa.

c. Excerpts of the 5' regions of *LAMA3* transcripts showing the start of the predicted open reading frames. The 5'UTR sequences are shown in lower case; and codons are shown in upper case with amino acid translation underneath.

Figure 4

Map of exon 39 of the *LAMA3* gene, showing the additional transcribed sequences compared to the previously reported mRNA sequence. A predicted TATA box is shown in bold type, identified by the TSSG and TSSW programs. The predicted start of transcription is shown in red. Primers used to map the transcription start site are shown as arrows. Primers P2F and P3F were found to amplify RT-PCR keratinocyte cDNA in combination with reverse primers in downstream exons, whereas P1F did not (data not shown).

Figure 5

The homozygous ancestral LOC mutation in exon 39 of *LAMA3* (151insG) shared by all affected persons in Families 1-14. In addition, the proband in Family 15 was heterozygous for this mutation.

a. Direct sequence of a *LAMA3* exon 39 PCR product from a normal control. Codons 49-53 of the *LAMA3A* transcript are shown.

b. Equivalent region as shown in (a) derived from the proband in LOC Family 1 (LOC patient 1-1, Fig. 2), showing homozygous insertion of G at position 151 (151insG in the *LAMA3A* transcript). This frameshift mutation leads to a premature termination codon 7 bp downstream of the insertion (not seen here).

c. Equivalent region as shown in (a) derived from the father of the proband in LOC Family 1. Overlapping sequence traces can be seen due to heterozygosity for the insertion mutation.

d. Equivalent region as shown in (a) derived from the mother of the proband in LOC Family 1. Again, overlapping sequence traces can be seen due to heterozygosity for the 151insG mutation.

Figure 6

Compound heterozygous mutation in the proband from LOC Family 15. This patient was heterozygous for the shared haplotype at the LOC locus (Fig. 2) and was subsequently found to be heterozygous for the 151insG mutation (data not shown).

a. Direct sequence of a *LAMA3* exon 60 PCR product from a normal control. Codons 941-945 of the *LAMA3A* transcript are shown. Box indicates arginine codon 943.

b. Equivalent region as shown in (a) derived from the proband in LOC Family 15 (LOC patient 15-1, Fig. 2), showing heterozygous nonsense mutation R943X (boxed).

c. Mutation R943X destroys a single *Sal* I restriction enzyme site present in the exon 60

PCR fragment. Lane 1 shows undigested 335 bp exon 60 PCR product. Lanes 2-3 show Sal I digests of exon 60 PCR products derived from the mother, father and proband of Family 15, respectively. The father's DNA digests fully, giving bands of 230 and 105 bp (lane 3). In contrast, both the mother and the proband's DNA show an additional undigested 335 bp band due to the mutation. Thus, the R943X mutation was inherited maternally, consistent with the haplotype data (Fig. 2).

Figure 7

Mutant *LAMA3A* transcript escapes nonsense-mediated mRNA decay.

a. Direct sequencing of a *LAMA3A*-specific RT-PCR product generated with primers L3AP3F and L3AP4R (Table 1) derived from epidermal mRNA from an LOC heterozygote. The forward L3AP3F sequence beginning at codon 49 (TGC) is shown. Heterozygosity for the 151insG mutation is clearly seen as overlapping sequence traces.

b. Direct sequencing of a *LAMA3* exon 39 genomic PCR product derived from the same individual as in (a), also sequenced with primer L3AP3F. Note that the heterozygous bases are very similar in signal intensity between the cDNA and genomic DNA samples, for example, where indicated by arrows in each case. Thus, there is no appreciable decay of the mutant message.

c. Genomic sequence in the region of exon 45, downstream of the LOC mutation 151insG in exon 39. The first two in-frame ATG codons that follow the mutation are shown in bold. The first of these, methionine codon 218 is a poor match for the Kozak consensus sequence, a feature required for eukaryotic translation initiation (shown above with matching bases boxed). In contrast, the next ATG, codon 227, is a perfect match for the Kozak sequence (boxed). Therefore, it was predicted that translation might take place from ATG codon 227, leading to an N-terminal truncation of 226 amino acids. Efficient translation of the mutant transcript would prevent nonsense-mediated mRNA decay.

Figure 8

Radioimmunoprecipitation of [^{35}S]-labelled secreted proteins from control and LOC keratinocytes with laminin 5 monoclonal antibody K140. Approximate molecular weight values are shown (in kDa). Lane 1, immunoprecipitation from control keratinocytes showing two high molecular weight bands, assumed to be the laminin α3a and α3b isoforms (marked a & b). Laminin α3a normally migrates at ~165 kDa on SDS-gels (20). The upper band could also be due to co-immunoprecipitation of other laminin alpha chains. Lower bands may include the laminin β3 and γ2 chains and other associated proteins. Lane 2, immunoprecipitation from LOC keratinocytes, showing a size reduction in the presumptive laminin α3a band (marked Δa), of approximately 24 kDa, the size predicted by loss of the N-terminal 226 amino acids. The fainter levels of the deleted α3a and the α3b bands in the LOC sample are likely to be because the LOC keratinocyte culture was much less confluent than the normal control. These results were replicable but lack of LOC cells prevented further labelling experiments to adjust loading.

Figure 9

Indirect immunofluorescence staining of LOC skin (panels a & c), compared to normal control skin (panels b & d). Monoclonal antibodies used were GB3 against the laminin 5 trimer (a & b) and K140 against laminin β3 (c & d). No significant changes in the intensity or distribution of staining was seen between the samples, showing that the mutated laminin α3a chain is capable of assembly and secretion, confirming the immunoprecipitation data (Fig. 8).

Figure 10

Electron microscopy of a skin biopsy from the proband in LOC Family 1. The ultrastructure of the dermal-epidermal junction (DEJ) was generally normal, but there were some qualitative changes. The number of hemidesmosomes (HD) and anchoring fibrils (AFB) appear normal. However, some of the hemidesmosome plaques are small and lack normal sub-basal dense plates (HDs). These diminutive cell-stromal junctions are associated with reduced numbers of anchoring filaments (AFL) and focal widening (*) of the lamina lucida (LL), although the lamina densa (LD) appeared normal. There are no frank splits in the lamina lucida, as would be expected in the junctional forms of epidermolysis bullosa to laminin 5 ablation mutations, where anchoring filaments are absent.

Figure 1 Clinical features of LOC syndrome

Figure 9

Immunohistochemistry

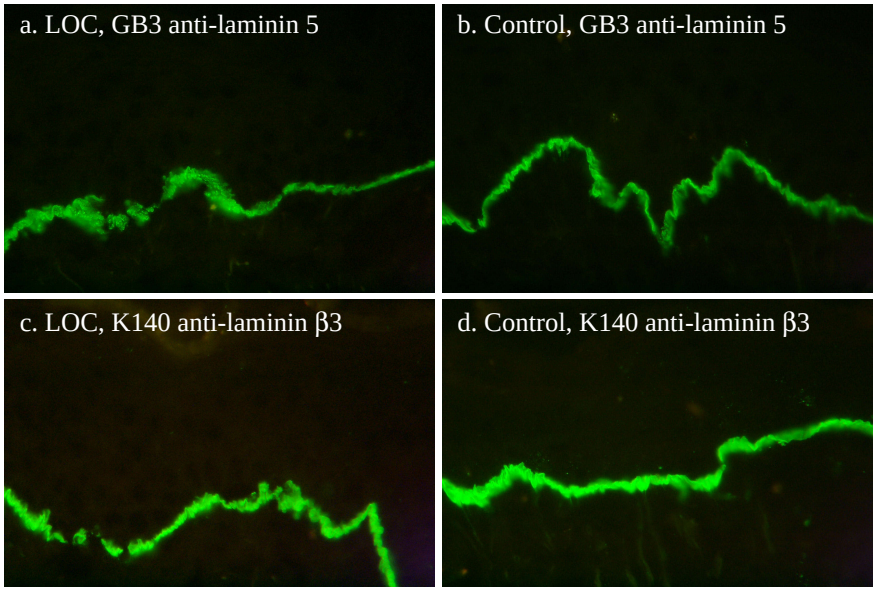

Figure 8

Laminin α3 IP

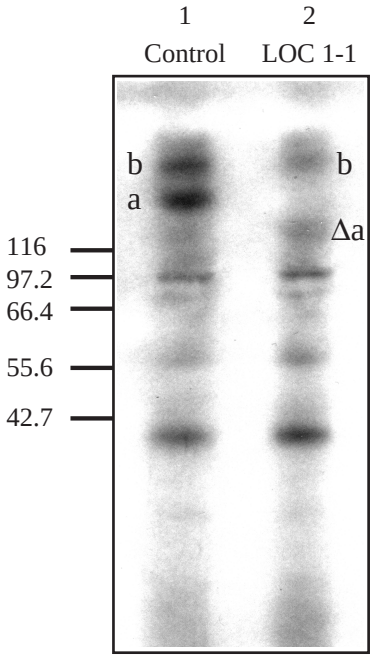

Figure 7

a. RT-PCR heterozygote

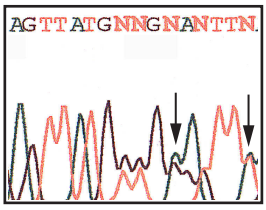

b. Genomic DNA

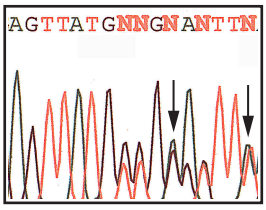

c. Potential *LAMA3A* exon 45 initiation sites

```
...cccacagcacatttgcctttgattgtggcccctaca

                    GCC RCC ATG G
gAT TGC GAC AGC TGT GTG ATG ACC CTC CTG
     C   D   S   C   V   M   T   L   L

              GCC RCC ATG G
AAC GAC CTG GCC ACC ATG GGC GAG CAG CTC
 N   D   L   A   T   M   G   E   Q   L

CGC CTG GTC AAG TCT CAG CTG CAG GGC CTG
 R   L   V   K   S   Q   L   Q   G   L

AGT GCC AGC GCA GGG CTT CTG GAG CAG ATG
 S   A   S   A   G   L   L   E   Q   M

AGG CAC ATG GAG ACC CAG GCC AAG GAC CTG
 R   H   M   E   T   Q   A   K   D   L

AGG gtaaatcccctgcggccgagagtagacacgtg...
 R
```

Figure 6

Compound heterozygote mutation in Family 15

a. LAMA3 control sequence

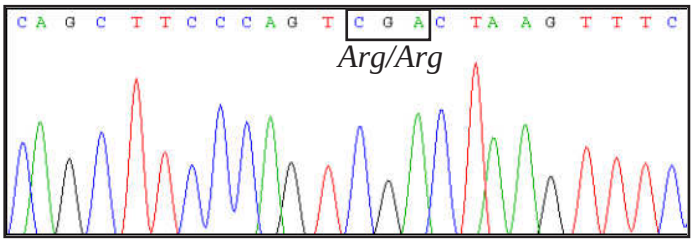

b. LOC patient 15-1

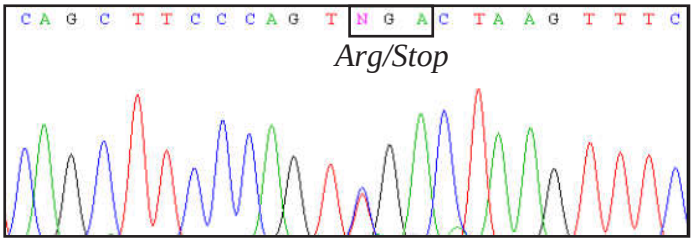

c. Family 15, *Sal* I digests

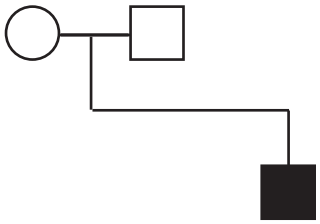

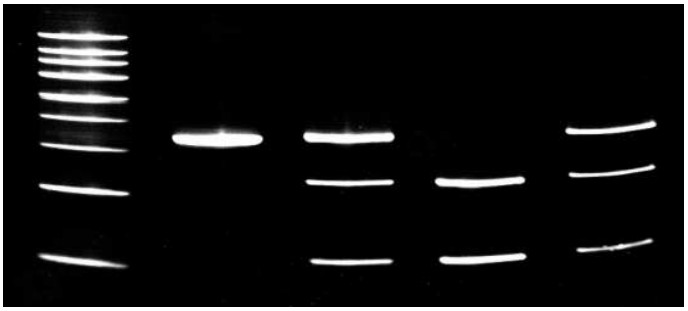

Figure 5

Exon 39 mutation in LOC

a. *LAMA3* exon 1 control sequence

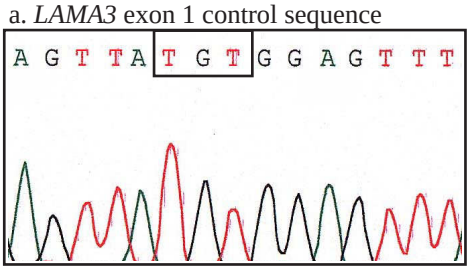

b. LOC patient 1-1, homozygous 151insG

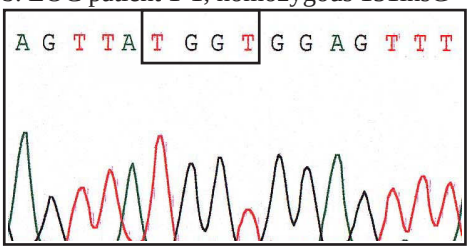

c. Father of LOC patient 1-1

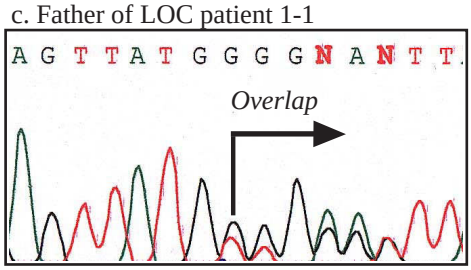

d. Mother of LOC patient 1-1

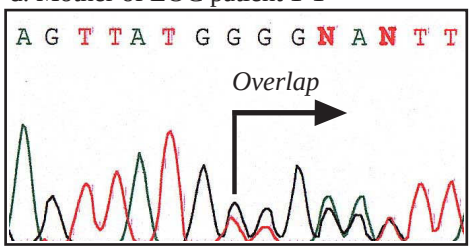

Figure 4

Mapping the *LAMA3A* transcription start site

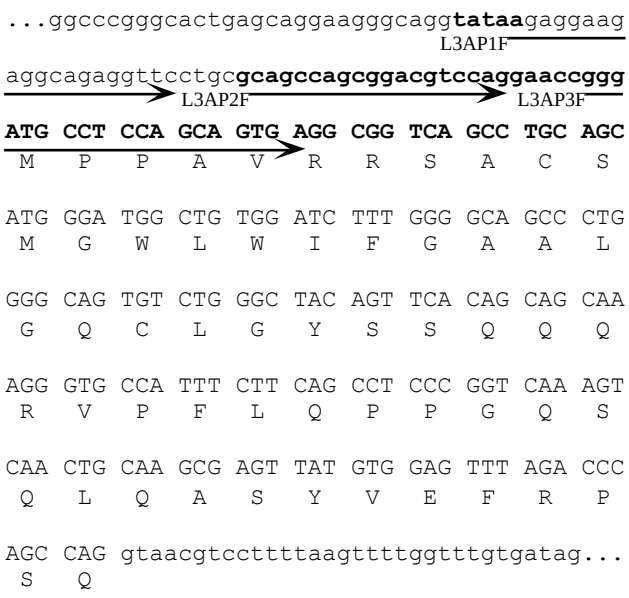

Figure 3

a. *LAMA3* intron-exon organization

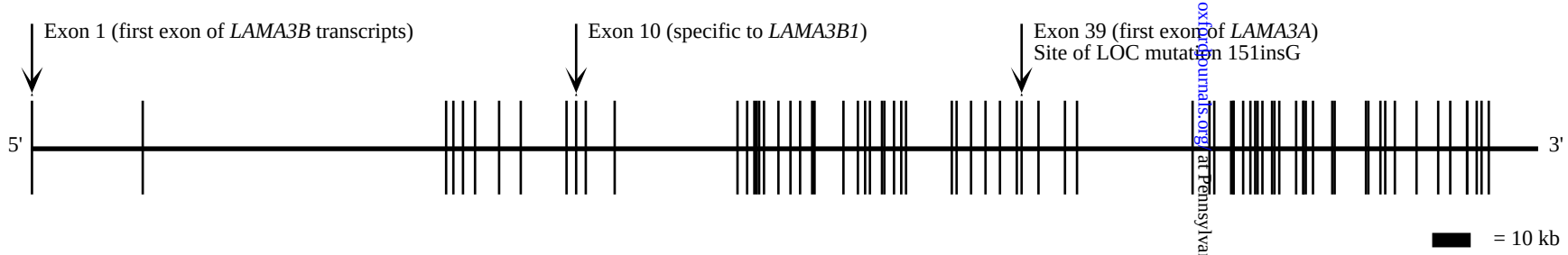

b. *LAMA3* transcripts/isoforms

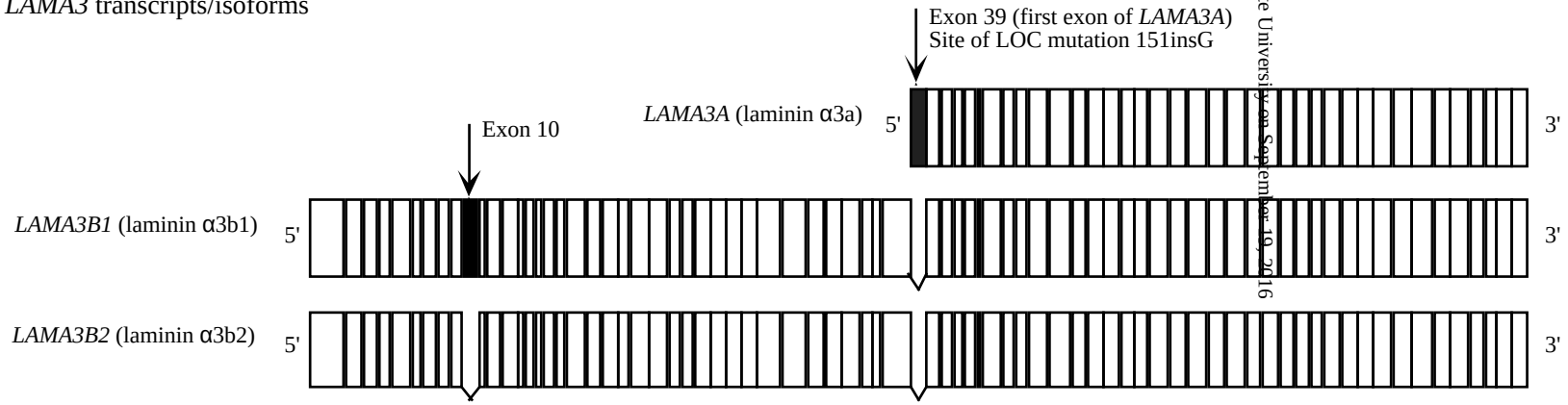

c. *LAMA3* transcripts/isoforms initiation codons:

LAMA3A: `... ggg acc ggg ATG CCT CCA...`
`M P P`

LAMA3B1/B2: `... cgc ggc tgg ATG GCG GCG...`
`M A A`

Figure 2

a. Pedigrees of consanguineous LOC families used in genome screen

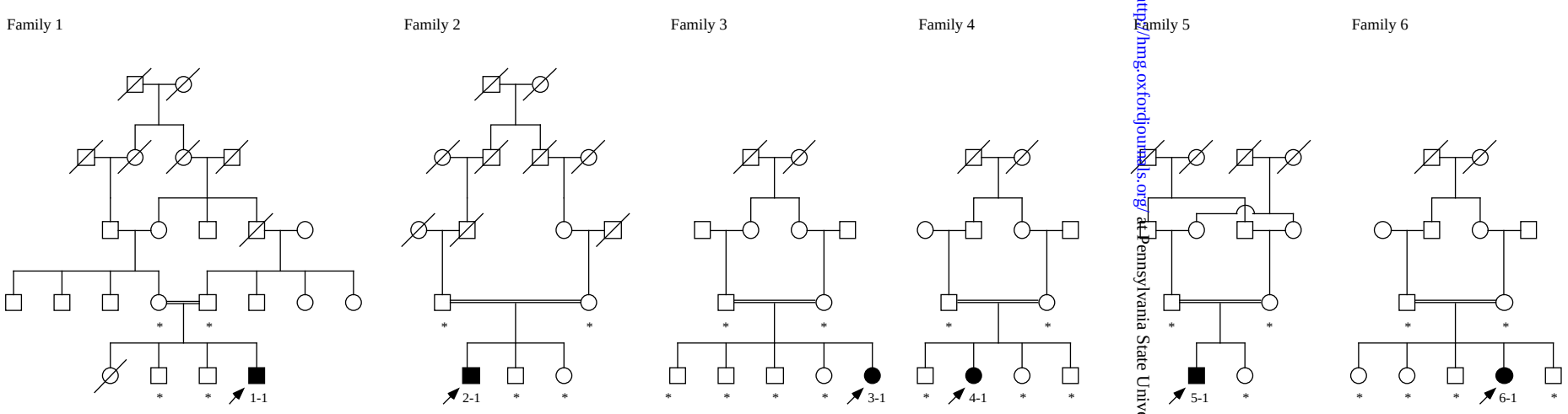

b. Genotypes for markers at the LOC locus in all affected persons studied

	LOC families of known consanguinity								Non-consanguineous LOC families									
LOC Family/Patient:	1-1	2-1	3-1	4-1	5-1	6-1	7-1	7-2	8-1	9-1	9-2	10-1	10-2	11-1	12-1	13-1	14-1	15-1
Marker																		
D18S453	150,162	150,160	150,158	160,160	160,160	156,156	154,160	150,160	154,154	150,160	150,150	162,162	162,162	158,158	160,160	256,256	150,150	150,156
D18S1149	268,268	258,268	268,268	258,258	268,268	262,262	268,268	268,268	268,268	268,268	268,268	268,268	268,268	268,268	268,268	266,266	268,268	268,258
D18S1104	155,155	155,163	155,155	159,159	155,155	155,155	155,155	155,155	155,155	155,155	155,155	155,155	155,155	155,155	155,155	153,153	155,155	155,161
D18S869	195,195	195,203	195,195	195,195	195,195	195,195	195,199	195,195	195,195	195,195	195,195	195,195	195,195	195,195	195,195	195,195	195,195	195,183
LAMA3GT1	**290,290**	**290,290**	**290,290**	**290,290**	**290,290**	**290,290**	**290,290**	**290,290**	**290,290**	**290,290**	**290,290**	**290,290**	**290,290**	**290,290**	**290,290**	**290,290**	**290,290**	**290**,290
LAMA3GT2	**195,195**	**195,195**	**195,195**	**195,195**	**195,195**	**195,195**	**195,195**	**195,195**	**195,195**	**195,195**	**195,195**	**195,195**	**195,195**	**195,195**	**195,195**	**195,195**	**195,195**	**195**,193
D18S1101	**281,281**	**281,281**	**281,281**	**281,281**	**281,281**	**281,281**	**281,281**	**281,281**	**281,281**	**281,281**	**281,281**	**281,281**	**281,281**	**281,281**	**281,281**	**281,281**	**281,281**	**281**,285
D18S480	129,129	133,137	137,137	137,137	137,137	137,137	137,137	137,137	137,137	137,137	137,137	129,129	129,129	137,137	133,137	137,137	137,137	137,129
D18S1107	96,96	84,96	84,84	84,84	84,84	84,84	84,84	84,84	84,84	84,84	84,84	96,96	96,96	84,84	84,94	84,84	84,84	84,96
D18S478	246,246	246,256	246,250	246,246	246,246	246,246	246,250	246,246	246,246	246,256	256,256	250,250	250,250	250,250	250,260	250,250	250,250	250,256

Figure 10

Ultrastructure of LOC dermal-epidermal junction